

# CO Catalytic Oxidation on Iron-Embedded Graphene: Computational Quest for Low-Cost Nanocatalysts

Yafei Li,<sup>†</sup> Zhen Zhou,<sup>†,\*</sup> Guangtao Yu,<sup>‡</sup> Wei Chen,<sup>§</sup> and Zhongfang Chen<sup>§,\*</sup>

*Institute of New Energy Material Chemistry, Nankai University, Tianjin 300071, People's Republic of China, The State Key Laboratory of Theoretical and Computational Chemistry, Institute of Theoretical Chemistry, Jilin University, Changchun 130023, People's Republic of China, and Department of Chemistry, Institute for Functional Nanomaterials, University of Puerto Rico, Rio Piedras Campus, San Juan, Puerto Rico 00931*

Received: December 4, 2009; Revised Manuscript Received: January 24, 2010

The catalytic oxidation of CO on Fe-embedded graphene was investigated by means of first-principles computations. Fe atom can be constrained at a vacancy site of graphene with a high diffusion barrier (6.78 eV), and effectively activate the adsorbed O<sub>2</sub> molecule. The reactions between the adsorbed O<sub>2</sub> with CO via both Langmuir–Hinshelwood (LH) and Eley–Rideal (ER) mechanisms were comparably studied. The Fe-embedded graphene shows good catalytic activity for the CO oxidation via the more favorable ER mechanism with a two-step route.

## 1. Introduction

The low-temperature oxidation of carbon monoxide (CO) plays an important role in solving the growing environmental problems caused by CO emission from automobiles, industrial processes, etc. CO oxidation, often quoted as a textbook example of catalytic reaction, is one of the most extensively investigated reactions in heterogeneous catalysis.<sup>1–26</sup> Though some noble metals, such as Pd,<sup>1</sup> Pt,<sup>2</sup> and Rh,<sup>3</sup> can effectively catalyze CO oxidation, these noble metal catalysts usually require high reaction temperature for efficient operation.<sup>4</sup> Thus, scientists continuously seek suitable catalysts to realize the low-temperature oxidation of CO.<sup>21–27</sup>

Nanocatalysis, one of the most exciting subfields of the emerging nanoscience, is promising to bring us breakthroughs. Intrinsically associated with low dimensionality, some noble metal clusters show excellent catalytic behaviors clearly distinguished from those of their bulk forms. For example, although bulk gold has long been thought to be catalytically inactive, free<sup>5–9,28</sup> and especially metal oxide supported<sup>10–17,20</sup> Au clusters exhibit rather high catalytic activity for CO oxidation. It was revealed that not only the size of gold clusters but also the choice of the oxide support substantially affects the catalytic activity of Au clusters. Obviously, besides “size effect”, the “support effect” has to be considered for rational design of superior nanocatalysts.

As a novel form of carbon, graphene is a promising candidate as the support for metal atoms and clusters to realize new carbon–metal nanocomposite catalysts, since the unique long-range  $\pi$ -conjugated structure brings graphene outstanding thermal, mechanical, and electrical properties.<sup>29–34</sup> For example, graphene shows the largest strength ever measured,<sup>29</sup> it is chemically stable and inert, and its ability to conduct electricity is better than that of any other known material at room temperature.<sup>30,35</sup> Moreover, the huge surface-to-volume ratio is

also advantageous for graphene as a support for heterogeneous catalysts. Very recently, Yoo et al.<sup>18</sup> demonstrated experimentally that small Pt clusters supported on graphene sheets exhibit high catalytic activity for CO oxidation, and graphene sheets display a remarkable modulation to the catalytic performances of Pt clusters. On the theoretical side, Lu et al.<sup>19</sup> predicted that Au-embedded graphene is a highly active catalyst for CO oxidation, which can be attributed to the partially occupied d orbital localized in the vicinity of the Fermi level due to the interaction of the Au atom with graphene. These experimental and theoretical investigations provide strong evidence that graphene is an attractive catalyst support that can display unusual behaviors compared with traditional supports.

Although some noble metal (Pt, Au, Pd, etc.) based catalysts are effective for CO oxidation, they are costly and limited in nature, which hampers their more general use in large-scale production. Consequently, researchers devoted great effort to developing low-cost and high-activity non noble metal based catalysts, such as Fe<sub>x</sub>O<sub>y</sub><sup>36,37</sup> and Co<sub>x</sub>O<sub>y</sub>.<sup>21,38,39</sup> The recent progress is rather encouraging. Xie et al.<sup>21</sup> demonstrated that Co<sub>3</sub>O<sub>4</sub> nanorods have surprisingly high catalytic activity for CO oxidation at very low temperature (–77 °C). Via a joint experimental and theoretical study, Xue et al.<sup>36</sup> revealed that iron oxides can serve as good catalysts for CO oxidation. Nigam and Majumder<sup>40</sup> proposed theoretically that Fe atom and small clusters encapsulated with BN fullerene cage are active and stable catalysts for CO oxidation.

In this work, we performed first-principles computations to explore the catalytic performance of non noble metal Fe-embedded graphene for CO oxidation. It is the unique characteristics of Fe that prompted us to choose it: inexpensive, environmentally benign, readily available, and rich in the earth, almost meeting all the requirements to develop low-cost, green, and efficient catalysts. Since Au-embedded graphene shows high catalytic activity for CO oxidation,<sup>19</sup> it is natural to expect that Fe-embedded graphene can also exhibit similar catalytic behavior due to the interaction between the Fe atom and graphene. Several theoretical studies have been performed on metal–graphene composites;<sup>41–46</sup> however, only electronic and mag-

\* Corresponding authors. E-mail: zhouzhen@nankai.edu.cn (Z.Z.); zhongfangchen@gmail.com (Z.C.).

<sup>†</sup> Nankai University.

<sup>‡</sup> Jilin University.

<sup>§</sup> University of Puerto Rico.

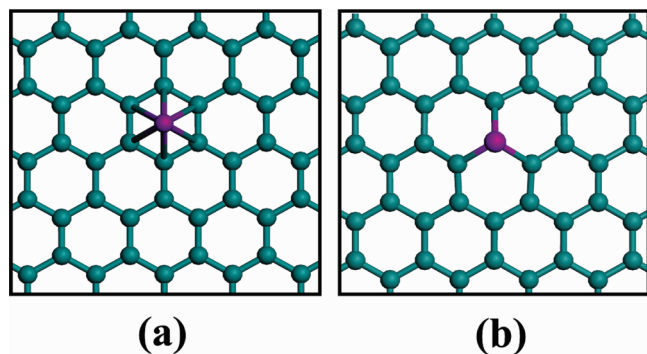


**Figure 1.** Typical atomic configurations for Fe adsorption on (a) the top of hexagonal site of pristine graphene, and (b) the vacancy site of graphene. The green and purple balls denote carbon and iron atoms, respectively.

netic properties were examined. To the best of our knowledge, the present study is the first focusing on the catalytic activity of non noble metals supported on graphene for the CO oxidation.

## 2. Computational Method

Our spin-unrestricted density functional theory (DFT) computations were carried out through an all-electron method within a generalized gradient approximation (GGA) for the exchange-correlation term, as implemented in the DMol<sup>3</sup> code.<sup>47</sup> The double numerical basis set including the d-polarization functions (DND) basis set and PW91<sup>48</sup> functional was adopted. Self-consistent field (SCF) calculations were performed with a convergence criterion of  $10^{-6}$  au on the total energy. To ensure high-quality results, the real-space global orbital cutoff radius was chosen as high as 4.6 Å in the computations. All simulations were performed for a  $7 \times 7$  graphene supercell, which includes 98 carbon atoms. The Brillouin zone was sampled with  $2 \times 2 \times 1$   $k$  points. The transition states were located through the synchronous method with conjugated gradient refinements.<sup>49</sup> This method involves linear synchronous transit (LST) maximization, followed by repeated conjugated gradient (CG) minimizations, and then quadratic synchronous transit (QST) maximizations and repeated CG minimizations until a transition state is located.

## 3. Results and Discussion

**3.1. Searching for Fe-Embedded Graphene with High Diffusion Barrier.** We started our study by investigating the adsorption of one Fe atom on pristine graphene. Here the Fe adsorption energy is defined as  $E_{\text{ad}}(\text{Fe}) = E_{\text{tot}}(\text{graphene-Fe}) - E_{\text{tot}}(\text{graphene}) - E_{\text{tot}}(\text{Fe})$ , where  $E_{\text{tot}}(\text{graphene-Fe})$ ,  $E_{\text{tot}}(\text{graphene})$ , and  $E_{\text{tot}}(\text{Fe})$  are the total energies of one Fe atom embedded graphene, the graphene layer, and the free Fe atom in its ground state (quintet), respectively. Among the representative adsorption sites, including the hollow site (H) above the center of the hexagon, the bridge site (B) over a C–C bond, and the top site (T) directly above one C atom, the Fe atom prefers the H-site with an adsorption energy of 0.98 eV (Figure 1a). There is about 0.27|e| charge transfer from the Fe atom to graphene according to the Mulliken charge population analysis, and the whole system has a 2.07  $\mu_{\text{B}}$  magnetic moment, which is less than that of the free Fe atom (4  $\mu_{\text{B}}$ ). The above results agree well with the previous report by Santos et al.<sup>41</sup> However, being aware of the possible clustering problem of metal atoms on supports, a typical bottleneck for many proposed hydrogen storage materials,<sup>50</sup> we carefully computed the energy barrier for Fe diffusion on graphene from one H-site to its neighboring

one (Supporting Information, Figure S1). The rather small diffusion barrier (0.66 eV) indicates that the Fe adatom can easily diffuse on pristine graphene; thus the clustering problem arises. The small diffusion barrier may come from the uniform charge distribution on pristine graphene. Therefore, pristine graphene is not the ideal substrate for the Fe adatom to develop stable catalysts.

To conquer this bottleneck, we carved a vacancy on graphene, and then put one Fe atom on the top of the vacancy site (Figure 1b). Carbon vacancies or dangling bonds of carbon atoms can improve the stability of supported metal clusters or atoms on graphene, and tune the electronic structure of the corresponding clusters or atoms. Note that experimentally the existence of a vacancy was confirmed in graphene,<sup>18</sup> and the metal atom embedded graphene structures have been realized.<sup>51</sup> When an Fe atom is placed above a vacancy in graphene, it moves outward the plane of graphene after geometry optimization. Compared with the case of Fe-embedded pristine graphene (0.27|e|), Fe atom at the graphene vacancy site carries more positive charge (0.42|e|), and the whole system is nonmagnetic, which indicates a much stronger interaction between the Fe atom and the vacancy in graphene. Indeed, our computations showed that Fe forms strong covalent bonds with carbon atoms around the vacancy (Figure 1b). The dramatically enhanced adsorption energy (−7.87 eV) is quite close to that reported by Krashennnikov et al.<sup>44</sup> The diffusion of Fe on graphene from the vacancy site to its neighboring H-site is endothermic by 5.71 eV, and the computed energy barrier (6.78 eV) is much higher than that (0.66 eV) on pristine graphene, which vigorously excludes the clustering problem.

To gain deeper insight into the significant enhancement of Fe adsorption at the graphene vacancy site, we plotted the total density of states (TDOS) and projected density of states (PDOS) for graphene with a vacancy and an Fe adatom at the graphene vacancy site. The DOS of graphene with a vacancy is characterized with a sharp peak at the Fermi level (Figure 2a), which is obviously different from the case of pristine graphene: the DOS at the Fermi level is nearly zero. The PDOS analysis reveals that this sharp peak mainly originates from the states of carbon atoms around the vacancy site. Clearly, the dangling-bond states of the undercoordinated carbon atoms around the vacancy give rise to the sharp peak. However, in the DOS of Fe-embedded graphene (Figure 2b), the peak at the Fermi level disappears, and strong hybridization between 3d states of Fe and 2p states of graphene can be observed both above and below the Fermi level. This indicates that the Fe atom can use its valence electrons to saturate the dangling-bond states of the vacancy in graphene. Moreover, the strong hybridization fulfills the non-bonding 3d orbitals of Fe and eliminates its magnetism.

**3.2. Adsorption of CO and O<sub>2</sub> on Fe-Embedded Graphene.** We computed the interactions of O<sub>2</sub> and CO with Fe-embedded graphene, respectively. For O<sub>2</sub> adsorption on Fe-embedded graphene, the most energetically favorable configuration (Figure 3a) is characterized by O<sub>2</sub> parallel to the graphene surface forming two chemical bonds with Fe atom (side-on), and the adsorption energy is −1.65 eV, which is 0.25 eV more favorable than that of the end-on configuration. In comparison, O<sub>2</sub> usually adopts the end-on pattern on Au clusters.<sup>7</sup> There is about 0.4|e| charge transfer from Fe-embedded graphene to O<sub>2</sub>, which could occupy the antibonding  $2\pi^*$  orbitals of O<sub>2</sub> and subsequently lead to the elongation of the O–O bond from 1.21 to 1.39 Å, a typical value of peroxy species.<sup>52</sup> The strong hybridization between 3d states of Fe and 2p states of O<sub>2</sub> can be clearly seen from the computed DOS (Figure 2c). Note that the O<sub>2</sub> molecule

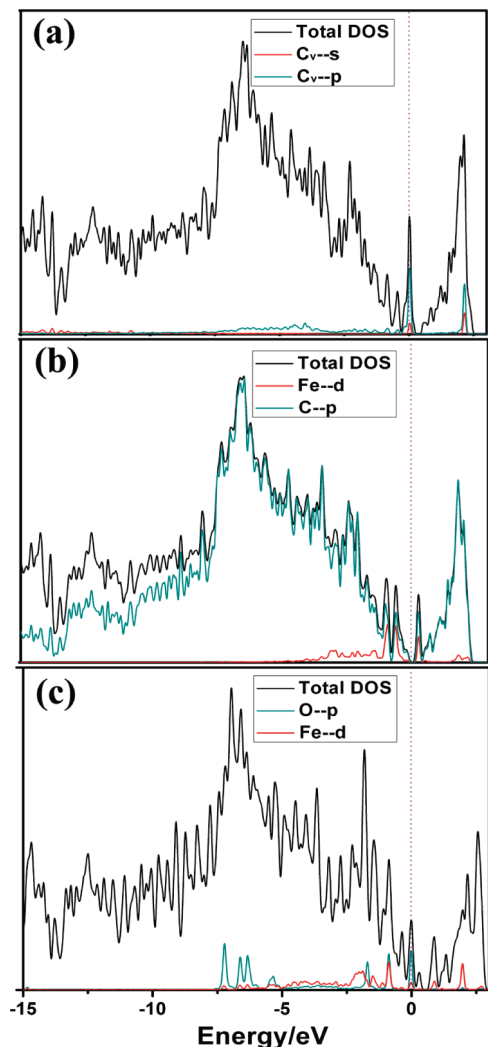


**Figure 2.** Computed total density of states (TDOS) and projected density of states (PDOS) for (a) graphene with a vacancy, (b) Fe adatom at the vacancy site of graphene, and (c) O<sub>2</sub> adsorption on Fe-embedded graphene.

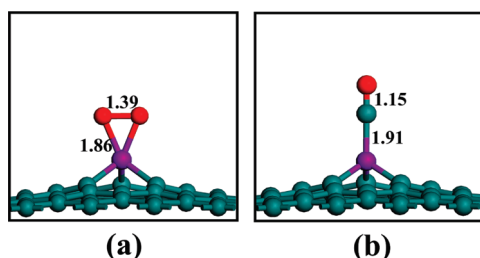


**Figure 3.** Optimized structures of (a) O<sub>2</sub> and (b) CO adsorption on Fe-embedded graphene. Oxygen atoms are denoted with red balls. Bond lengths are given in angstroms.

dissociates with a O–O distance up to 2.99 Å when interacting with a neutral Fe atom. However, when the Fe atom is constrained at the graphene vacancy, the dissociation pattern is not energetically favorable.

The end-on configuration (Figure 3b) is the lowest energy form for CO adsorbed on Fe-embedded graphene. The C–O bond length is nearly unchanged upon the adsorption. The computed CO adsorption energy (−1.38 eV) is also significant, but it is 0.27 eV less favorable than the case of O<sub>2</sub> adsorption.

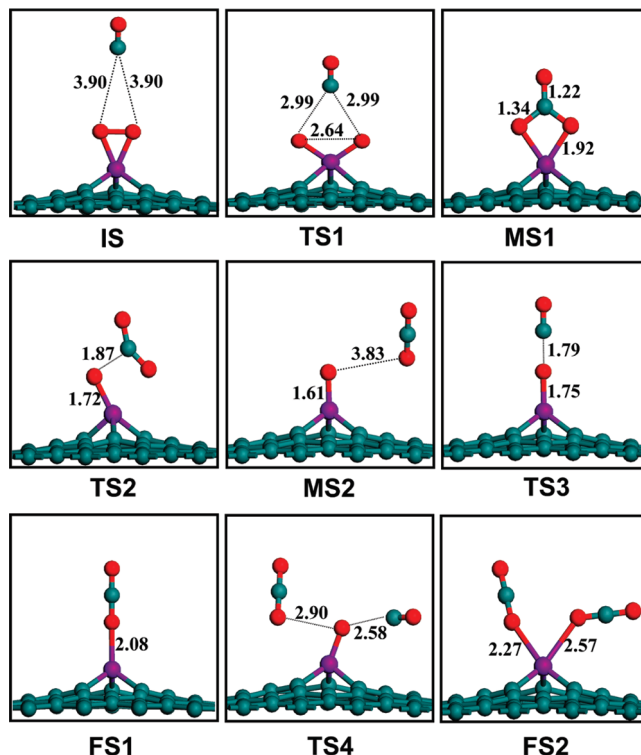


**Figure 4.** Atomic configurations of the initial state (IS), transition state (TS), intermediate state (MS), and final state (FS) for CO oxidation on Fe-embedded graphene.

The above results reveal that Fe-embedded graphene has strong interactions with O<sub>2</sub> and CO, but O<sub>2</sub> has even more favorable binding energies. Thus, we can expect that the Fe atoms at the graphene vacancy sites will be dominantly covered by the adsorbed O<sub>2</sub> molecules if CO/O<sub>2</sub> mixture is injected as the reaction gas, and consequently CO will react with O<sub>2</sub> on Fe-embedded graphene. The adsorbed O<sub>2</sub> is efficiently activated, which holds promise for further oxidation of CO.

**3.3. Mechanisms for the Reaction between the Adsorbed O<sub>2</sub> and CO.** Generally, there are two well-established mechanisms for the reaction of O<sub>2</sub> with CO, namely the Langmuir–Hinshelwood (LH) mechanism and the Eley–Rideal (ER) mechanism. The LH mechanism involves the coadsorption of O<sub>2</sub> and CO molecules before reaction, the formation of an intermediate state and desorption of CO<sub>2</sub> molecule. In the ER mechanism, the reactant CO molecules approach the already activated O<sub>2</sub>. In our study, both mechanisms were investigated comparably.

**Langmuir–Hinshelwood (LH) Mechanism.** Several coadsorption configurations via the LH mechanism (Supporting Information, Figure S2) were tested. Initially, O<sub>2</sub> and CO molecules were put at rather close sites. However, no CO<sub>2</sub> or O–O–CO intermediate state formation was found after full geometry optimizations. This indicates that the reaction process of CO oxidation on Fe-embedded graphene via the LH mechanism is almost impossible or proceeds with great difficulty. This conclusion is further enhanced when we consider the more favorable O<sub>2</sub> binding energies. Similarly, Nigam and Majumder argued that CO oxidation on Fe clusters encapsulated with BN cage cannot be initiated via the LH mechanism.<sup>40</sup> Therefore, in the following steps we emphasize the ER mechanism.

**Eley–Rideal (ER) Mechanism.** The atomic configurations at various states along the reaction path are displayed in Figure 4, and the corresponding energy profiles are summarized in Figure 5.

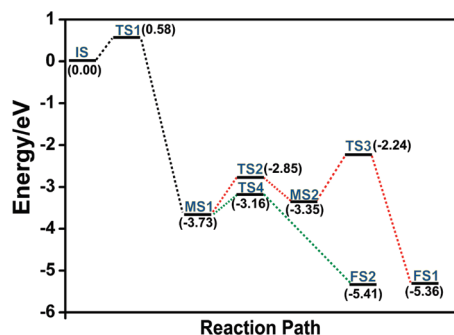


**Figure 5.** Energy profiles for CO oxidation over Fe on defective graphene. On the basis of MS1, two reaction paths are denoted with red and green dotted lines, respectively. The numbers in parentheses are relative energies referred to the reactants in electronvolts.

The configuration of physisorbed CO above O<sub>2</sub> preadsorbed on the Fe-embedded graphene was selected as the initial state (IS). When one CO molecule approaches the activated O<sub>2</sub>, CO can be inserted into the O–O bond to form a carbonate-like intermediate state CO<sub>3</sub> (MS1) on Fe adatom, where the O–O distance is further elongated to 2.15 Å. This is quite similar to the reaction of CO with O<sub>2</sub> on Au.<sup>2–7</sup> The process of CO insertion into the O–O bond is exothermic by 3.73 eV, but it is not barrier free, and a 0.58 eV energy barrier (TS1) should be overcome (Figure 5) due to the breaking of the O–O bond and the formation of new C–O bonds.

The reaction can proceed following two paths from MS1. In the first path, the CO<sub>2</sub> molecule in MS1 experiences an endothermic dissociation (by 0.38 eV) to form the residual intermediate state (MS2) crossing a relatively high energy barrier of 0.88 eV (TS2), followed by the step that the O atom bound with Fe atom in MS2 reacts with a second CO molecule to produce CO<sub>2</sub> (FS1). Although the step from MS2 to FS1 is exothermic by 2.01 eV, it has an even higher energy barrier of 1.11 eV (TS3), which could be attributed to the strong binding between Fe and O (−4.99 eV). The produced CO<sub>2</sub> molecule is bound to Fe via an O atom with a −0.42 eV adsorption energy, which can be easily overcome by the energy released in this process, thus facilitating its desorption.

The second reaction path involves the process that MS1 reacts with another CO molecule to produce two CO<sub>2</sub> molecules (FS2) with a energy barrier of 0.57 eV (TS4). Both of the produced CO<sub>2</sub> molecules in FS2 are bound to Fe with O atoms with the average adsorption energy of −0.23 eV/CO<sub>2</sub>. Since the energy released in this step (1.68 eV) can sufficiently surmount the adsorption energy, the desorption of these two CO<sub>2</sub> molecules from FS2 would be rather flexible. Overall, the second path is more thermally favorable and has a more modest energy barrier, and it should be more preferred under experimental conditions.

#### 4. Conclusion

In summary, we performed first-principles computations to investigate the reaction of carbon monoxide with oxygen on Fe embedded in graphene, aiming to explore the catalytic activity of graphene–metal systems. Vacancies in graphene can efficiently enhance the Fe adsorption and result in a 6.78 eV diffusion barrier. Due to the strong hybridization between 3d states of Fe and the 2p state of O<sub>2</sub>, O<sub>2</sub> can be efficiently activated by Fe adatom, and then CO can be inserted into the elongated O–O bond to form a carbonate-like intermediate state CO<sub>3</sub> with a moderate energy barrier (0.58 eV) via the Eley–Rideal mechanism. Then, CO<sub>3</sub> reacts with another CO to produce two CO<sub>2</sub> molecules also with a rather modest energy barrier (0.57

eV). Our results demonstrate that Fe-embedded graphene has good catalytic activity for CO oxidation. We hope that this study will promote further experimental and theoretical efforts to design novel catalysts based on metal–graphene systems.

**Acknowledgment.** Support in China by NSFC (20873067) and NCET, and in the United States by NSF Grant CHE-0716718, the Institute for Functional Nanomaterials (NSF Grant 0701525), the U.S. Environmental Protection Agency (EPA Grant RD-83385601), and in part by the National Science Foundation through TeraGrid resources, is gratefully acknowledged. G. T. Yu thanks the startup fund (450080011085) from Jilin University.

**Supporting Information Available:** Energy profiles for Fe diffusion on pristine graphene, and optimized structures of coadsorbed O<sub>2</sub> and CO molecules on Fe-embedded graphene. This material is available free of charge via the Internet at <http://pubs.acs.org>.

#### References and Notes

- Zhang, C. J.; Hu, P. *J. Am. Chem. Soc.* **2001**, *123*, 1166.
- (a) Alavi, A.; Hu, P.; Deutsch, T.; Silvestrelli, P. L.; Hutter, J. *Phys. Rev. Lett.* **1998**, *80*, 3650. (b) Eichler, A.; Hafner, J. *Surf. Sci.* **1999**, *433*, 58.
- (a) Liu, Z. P.; Hu, P. *J. Chem. Phys.* **2001**, *115*, 4977. (b) Eichler, A. *Surf. Sci.* **2002**, *498*, 314.
- Oh, S. H.; Hoflund, G. B. *J. Catal.* **2007**, *245*, 35.
- Lopez, N.; Nørskov, K. *J. Am. Chem. Soc.* **2002**, *124*, 11262.
- Wallace, W. T.; Whetten, R. L. *J. Am. Chem. Soc.* **2002**, *124*, 7499.
- Socaciu, L. D.; Hagen, J.; Bernhardt, T. M.; Woste, L.; Heiz, U.; Häkkinen, H.; Landman, U. *J. Am. Chem. Soc.* **2003**, *125*, 10437.
- Kimble, M. L.; Castleman, A. W., Jr.; Mitrić, R.; Bürgel, C.; Bonacic-Koutecky, V. *J. Am. Chem. Soc.* **2004**, *126*, 2526.
- Hernández, N. C.; Sanz, J. F.; Rodriguez, J. A. *J. Am. Chem. Soc.* **2006**, *128*, 15600.
- (a) Haruta, M.; Kobayashi, T.; Samo, H.; Yamada, N. *Chem. Lett.* **1987**, *2*, 405. (b) Haruta, M.; Yamada, N.; Kobayashi, T.; Ijima, S. *J. Catal.* **1989**, *115*, 301. (c) Haruta, M.; Tsubota, S.; Kobayashi, T.; Kageyama, H.; Genet, M. J.; Delmon, B. *J. Catal.* **1993**, *144*, 175.
- (a) Grisel, R. J. H.; Nieuwenhuys, B. E. *J. Catal.* **2001**, *199*, 48. (b) Gluhoi, A. C.; Dekkers, M. A. P.; Nieuwenhuys, B. E. *J. Catal.* **2003**, *219*, 197.
- Liu, Z. P.; Hu, P.; Alavi, A. *J. Am. Chem. Soc.* **2002**, *124*, 14770.
- Yoon, B.; Häkkinen, H.; Landman, U.; Worz, A. S.; Antonietti, J.-M.; Abbet, S.; Judai, K.; Heiz, U. *Science* **2005**, *307*, 403.
- Zhang, C.; Yoon, B.; Landman, U. *J. Am. Chem. Soc.* **2007**, *129*, 2228.
- Wang, C. M.; Fan, K. N.; Liu, Z. P. *J. Am. Chem. Soc.* **2007**, *129*, 2642.
- Matthey, D.; Wang, J. G.; Wendt, S.; Matthiesen, J.; Schaub, R.; Lægsgaard, E.; Hammer, B.; Besenbacher, F. *Science* **2007**, *315*, 1692.
- Camellone, M. F.; Fabris, S. *J. Am. Chem. Soc.* **2009**, *131*, 10473.
- Yoo, E.; Okata, T.; Akita, T.; Kohyama, M.; Nakamura, J.; Honma, I. *Nano Lett.* **2009**, *9*, 2255.
- Lu, Y. H.; Zhou, M.; Zhang, C.; Feng, Y. P. *J. Phys. Chem. C* **2009**, *113*, 20156.
- (a) Haruta, M. *Catal. Today* **1997**, *36*, 153. (b) Sanchez, A.; Abbet, S.; Heiz, U.; Schneider, W.-D.; Häkkinen, H.; Barnett, R. N.; Landman, U. *J. Phys. Chem. A* **1999**, *103*, 9573. (c) Bond, G. C.; Thompson, D. T. *Catal. Rev.—Sci. Eng.* **1999**, *41*, 319.
- Xie, X.; Li, Y.; Liu, Z. Q.; Haruta, M.; Shen, W. *Nature* **2009**, *458*, 746.
- Moroz, B. L.; Pyrjaev, P. A.; Zaikovskii, V. I.; Bukhtiyarov, V. I. *Catal. Today* **2009**, *144*, 292.
- Rodríguez-González, V.; Zanella, R.; Calzada, L. A.; Gómez, R. *J. Phys. Chem. C* **2009**, *113*, 8911.
- Hellman, A.; Klacar, S.; Grönbeck, H. *J. Am. Chem. Soc.* **2009**, *131*, 16636.
- Wang, H. F.; Gong, X. Q.; Guo, Y. L.; Guo, Y.; Lu, G. Z.; Hu, P. *J. Phys. Chem. C* **2009**, *113*, 6124.
- Lim, S. H.; Phonthammachai, N.; Zhong, Z. Y.; Teo, J.; White, T. J. *Langmuir* **2009**, *25* (16), 9480.
- Min, B. K.; Friend, C. M. *Chem. Rev.* **2007**, *107*, 2709.
- Gao, Y.; Shao, N.; Bulusu, S.; Zeng, X. C. *J. Phys. Chem. C* **2008**, *112*, 8234.

- (29) Lee, G.; Wei, X.; Kysar, J. W.; Hone, J. *Science* **2008**, *321*, 385–388.
- (30) Zhang, Y.; Tan, Y.-W.; Stormer, H. L.; Kim, P. *Nature* **2005**, *438*, 201.
- (31) Ponomarenko, L. A.; Schedin, F.; Katsnelson, M. I.; Yang, R.; Hill, E. W.; Novoselov, K. S.; Geim, A. K. *Science* **2008**, *320*, 356.
- (32) Kan, E. J.; Li, Z. Y.; Yang, J. L. *NANO* **2008**, *3*, 433.
- (33) Berger, C.; Song, Z.; Li, X.; Wu, X.; Brown, N.; Naud, C.; Mayou, D.; Li, T.; Hass, J.; Marchenkov, A. N.; Conrad, E. H.; First, P. N.; Heer, W. A. d. *Science* **2006**, *312*, 1191.
- (34) Ci, L.; Xu, Z.; Wang, L.; Gao, W.; Ding, F.; Kelly, K.; Yakobson, B. I.; Ajayan, P. *Nano Res.* **2008**, *1*, 116.
- (35) Morozov, S. V.; Novoselov, K. S.; Katsnelson, M. I.; Schedin, F.; Elias, D.; Jaszczak, J. A.; Geim, A. K. *Phys. Rev. Lett.* **2008**, *100*, 016602.
- (36) Xue, W.; Wang, Z. C.; He, S. G.; Xie, Y.; Bernstein, E. R. *J. Am. Chem. Soc.* **2008**, *130*, 15879.
- (37) (a) Walker, J. S.; Straguzzi, G. I.; Manogue, W. H.; Schuit, G. C. A. *J. Catal.* **1988**, *110*, 299. (b) Uddin, M. A.; Komatsu, T.; Yashima, T. *J. Catal.* **1994**, *146*, 468. (c) Li, P.; Miser, D. E.; Rabiei, S.; Yadav, R. T.; Hajaligol, M. R. *Appl. Catal., B* **2003**, *43*, 151. (d) Xiong, Y.; Li, Z.; Li, X.; Hu, B.; Xie, Y. *Inorg. Chem.* **2004**, *43*, 6540. (e) Khedr, M. H.; Abdel Halim, K. S.; Nasr, M. I.; El-Mansy, A. M. *Mater. Sci. Eng., A* **2006**, *430*, 40. (f) Hu, C.; Gao, Z.; Yang, X. *Chem. Lett.* **2006**, *35*, 1288. (g) Zheng, Y.; Cheng, Y.; Wang, Y.; Bao, F.; Zhou, L.; Wei, X.; Zhang, Y.; Zheng, Q. *J. Phys. Chem. B* **2006**, *110*, 3093. (h) Szegedi, A.; Hegedüs, M.; Margitfalvi, J. L.; Kiricsi, I. *Chem. Commun.* **2005**, 1441. (i) Lin, H.; Chen, Y.; Wang, W. *J. Nanopart. Res.* **2005**, *7*, 249.
- (38) Jansson, J.; Palmqvist, A. E. C.; Fridell, E.; Skoglundh, M.; Österlund, L.; Thormählen, P.; Langer, V. *J. Catal.* **2002**, *211*, 387.
- (39) Saalfrank, J. W.; Maier, W. F. *Angew. Chem., Int. Ed.* **2004**, *43*, 2028.
- (40) Nigam, S.; Majumder, C. *ACS Nano* **2008**, *2*, 1422.
- (41) Santos, E. J. G.; Ayuella, A.; Fagan, S. B.; Filho, J.; Azevedo, D. L.; Souza Filho, A. G.; Sánchez-Porta, D. *Phys. Rev. B* **2008**, *78*, 195420.
- (42) Chan, K. T.; Neaton, J. B.; Cohen, M. L. *Phys. Rev. B* **2008**, *77*, 235430.
- (43) Sevinçli, C.; Topsakal, M.; Durgun, E.; Ciraci, S. *Phys. Rev. B* **2008**, *77*, 235430.
- (44) Krasheninnikov, A. V.; Lehtinen, P. O.; Foster, A. S.; Pyykkö, P.; Nieminen, R. M. *Phys. Rev. Lett.* **2009**, *102*, 126807.
- (45) Boukhvalov, D. W.; Katsnelson, M. I. *Appl. Phys. Lett.* **2009**, *95*, 023109.
- (46) Kim, G.; Jhi, S. H.; Lim, S.; Park, N. *Appl. Phys. Lett.* **2009**, *94*, 173102.
- (47) (a) Delley, B. *J. Chem. Phys.* **1990**, *92*, 508. (b) Delley, B. *J. Chem. Phys.* **2000**, *113*, 7756.
- (48) Perdew, J. P.; Wang, Y. *Phys. Rev. B* **1992**, *45*, 13244.
- (49) Govind, N.; Petersen, M.; Gitzgerald, G.; King-Smith, D.; Andzelm, J. *J. Comput. Mater. Sci.* **2003**, *28*, 250.
- (50) (a) Sun, Q.; Wang, Q.; Jena, P.; Kawazoe, Y. *J. Am. Chem. Soc.* **2005**, *127*, 14582. (b) Durgun, E.; Ciraci, S.; Zhou, W.; Yildirim, T. *Phys. Rev. Lett.* **2006**, *97*, 226102. (c) Li, S.; Jena, P. *Phys. Rev. Lett.* **2006**, *97*, 209601. (d) Yang, S. Y.; Yoon, M. N.; Wang, E.; Zhang, Z. Y. *J. Chem. Phys.* **2008**, *129*, 134707. (e) Krasnov, P. O.; Ding, F.; Singh, A. K.; Yakobson, B. I. *J. Phys. Chem. C* **2007**, *111*, 17977. (f) Li, M.; Li, Y. F.; Zhou, Z.; Shen, P. W.; Chen, Z. F. *Nano Lett.* **2009**, *9*, 1944.
- (51) Gan, Y.; Sun, L.; Banhart, F. *Small* **2008**, *4*, 587.
- (52) Gutsev, G. L.; Rao, B. K.; Jena, P. *J. Phys. Chem. A* **2000**, *104*, 11961.

JP911535V